J Mater Sci (2008) 43:7192–7202
DOI 10.1007/s10853-008-2989-z

A theory for yield phenomenon of glassy polymers based on the strain non-uniformity under loading conditions

G. Spathis

Received: 12 March 2008 / Accepted: 2 September 2008 / Published online: 23 October 2008

Abstract In this work, the yield phenomenon and its related features have been investigated under the concept of strain inhomogeneity, emerged inside the material during deformation processes. This strain non-uniformity in glassy polymers is either a direct consequence of the local microstructural density fluctuations existing in such materials or is the result of the manner by which the free volume is frozen in the glassy state. Assuming a simple strain density distribution function, the rate of plastic deformation can be extracted without any further assumption on a molecular conformational base or any other thermal activated process. The two model parameters required have a physical base related with the magnitude of the free volume and its fluctuation in glassy polymers. Appling this theory on the experimental results for three representative amorphous glassy polymers (PMMA, PS, and PC), all features of yield process, including strain softening effect, are easily described.

Introduction

Virtually all solid polymers, under certain conditions of temperature and strain rate, undergo a permanent shape change when subjected to a stress of sufficient magnitude. This plastic deformation, which is termed yielding, is accompanied in most cases by a stress softening followed by a strain hardening, when large deformation is applied especially on ductile materials. Moreover, the yield stress is sensitive to strain rate deformation, temperature and pressure conditions, and thermal history, properties which make the plastic phenomenon of polymers of great interest for experimental and theoretical analysis. Most of the work made in explaining these features is not restricted to the concept of continuous medium, and the subsequent kinematic formulation of plasticity theory. In contrast, the necessity of micromechanical description and deep inside on molecular behavior is obvious for obtaining an acceptable explanation of these effects [1–7]. In this trend, originally the BPA model [5] and later the work by Hasan and Boyce [6–8] illustrate many mechanical features of most representative glassy polymers such as PS, PMMA, and PC for various kinds of deformation modes and strain rate conditions. What is common in all these systematic works is the micromechanical model developed by Argon [3], which deals explicitly with intermolecular resistance to shear yielding. This analysis couples bond rotation (kink pair formation) to intermolecular energy calculated with continuum elasticity theory, and has the macroscopic yield stress related directly with temperature and strain rate. The Argon results closely resemble the Eyring [9] model, which considers plastic transformation as a thermal activated process; therefore, its special formulation leads to temperature and rate dependencies that are virtually indistinguishable from Eyring approach. The important conclusion that resistance to plastic deformation at the yield point is intermolecular in origin does not account however in an obvious way for strain softening. In order to overcome this shortcoming, BPA model [5] was developed on the base that Argon's concept of a thermal strength has been varied by an empirical equation as plastic deformation proceeds. In a more sophisticated way, Hasan and Boyce [7], trying to capture all plasticity features of amorphous

G. Spathis (✉)
School of Applied Mathematical and Physical Sciences,
Section of Mechanics, National Technical University of Athens,
5 Heroes of Polytechnion, 15773 Athens, Greece
e-mail: gspathis@central.ntua.gr

polymers including temperature treatments, developed a constitutive model, by considering a distribution in the activation energy barrier to deformation in a thermally activated model of yielding process. Even in this approach however they could not avoid semiempirical equations for time evolution of a set of internal variables introduced for the necessity of the proper description. Apart from these shortcomings, what is interesting in their analysis is that the plausible assumption of "pseudo-Gaussian" distribution of activated energy barriers is based on a similar distribution of the amount and size of free volume holes inside the substance of amorphous polymers. There was a strong historic association between yield and free volume concept, which is rejuvenated when positron annihilation lifetime spectroscopy (PALS) [8] was used to probe free volume in liquid and glassy polymers. PALS provides unique information about the properties of subnanometer size local free volume (holes) appearing due to the structural disorder in amorphous polymers [10]. This method is able to measure the mean value and the size distribution of these holes. By combining of this experimental evidence with, for example, pressure-volume-temperature experiments, the number of holes and their entire volume fraction can be estimated [11–14].

The plastic behavior of glassy polymers has been extensively and satisfactorily described by applying models based on thermally activated process. However, to overcome the shortcoming of explaining strain softening with the use of extra parameters and the variation with deformation, we will apply the concept of free volume to introduce a new mechanism of yielding. Following this trend, in this work, we will try to formulate in a plausible and simple way the idea of free volume fluctuation for a constitutive description of yield and post-yield phenomena of amorphous polymers. The way to reconcile the yield process with the free volume concept will be postulated on the assumption that not only the amount of free volume but also the state of its subdivision within the material plays a role in determining the corresponding properties. Based on this idea, which was first used by Hasan and Boyce as mentioned earlier, we will try to introduce a density distribution function for the imposed strain on the representative volume of deformed material. By this way, the strain inhomogeneity that accompanies plastic deformation will be taken into account, and the subsequent strain softening effect will be described. For obtaining such a result, we will avoid the common kinematic plastic formulation of multiple decomposition of deformational tensor, because such a description eliminates the advantage of strain inhomogeneous across the representative volume element. Instead of this approach, we will use the kinematic formulation introduced by Rubbin [15, 16], as has been done successfully by us in related previous works [17, 18]. The constitutive theory will be tested by comparing the results with the representative experimental work for amorphous polymers existing in bibliography.

Model for the free volume distribution

For many years, the glassy state and the melt of polymers have been considered to be homogeneous and random in structure. However, a lot of experimental results have been obtained that seem to indicate that the amorphous phase of polymers is not homogeneous on the microscopic level. Especially the small-angle X-ray scattering technique proved to be a convenient way of determining density fluctuation of amorphous polymers in liquid and glassy state, and its utility in the study of glassy polymer was first demonstrated by Wendorff and Fisher [19]. Curo and Roe [20], on the other hand, also utilized the technique of X-ray scattering to correlate the change of the specific volume with that in the density fluctuation, for three widely used polymers (PS, PMMA, and PC). Based on their experimental results, Curo and Roe [21] derived an equation, which relates explicitly the density fluctuation of glassy state with the free volume fraction (or hole volume) in amorphous polymers. By taking into account the value of 0.025 for the free volume fraction (as it is calculated for most polymers through the WLF [22] equation), they estimate the cavity size in glassy polymers ≈ 0.5 nm in diameter, which agrees reasonably well with data on the positron annihilation and ultrasonic velocity obtained by Mathotra and Pethrick [23, 24]. Based on the above-mentioned results, it is plausible to assume that inside the matrix of amorphous polymers, free volume, constituted from holes of varying sizes, is randomly distributed around polymer molecules. The question is if it is possible to extract a probability density function expressing the way in which the total amount of free volume is distributed inside the material matrix.

Following the experimental evidence provided by PALS, a semiempirical relation of the lifetime τ_3 of orthopositronium and the radius R of a spherical PALS free volume hole is widely known [25]:

$$\tau_3 = \frac{1}{2}\left(1 - \frac{R}{R_0} + \frac{1}{2\pi}\sin\frac{2\pi R}{R_0}\right)^{-1} \quad (1)$$

where $R_0 = R + \delta R$ with δR expressing the thickness of an electron layer on the wall of a hole, estimated to be equal to 0.166 nm. In the same experimental method (PALS), a continuous distribution of the inverse of the longest lifetime $\xi(1/\tau_3)$ can be obtained by analyzing the PALS spectra, which leads to the radius distribution $f(R)$ as:

$$f(R) = 2\delta R\left[\cos\frac{2\pi R}{R+\delta R} - 1\right]\frac{\xi(1/\tau_3)}{(R+\delta R)^2} \quad (2)$$

Then it is possible to obtain the free volume distribution as:

$$g(V) = \frac{f(R)}{4\pi R^2} \quad (3)$$

This distribution function in a series of amorphous glassy polymers [25] manifests certain features of the materials, such as synthesis, curing schedule, thermal treatment, and in all cases is expressed mainly with one characteristic peak.

In the sequel, an attempt will be presented to extract this free volume distribution function, based on a statistical ensemble in thermodynamic equilibrium, as the polymeric glass above T_g, assuming that its possible energy states follow a Boltzmann distribution.

Considering the macromolecules of an amorphous polymeric glassy in the liquid state, it is assumed that under a state of random thermal motion, some of these molecules may pull apart in such a way as to open a void or a hole in the liquid.

As a crude model, it is assumed that each piece of free volume comes in a spherical shape of radius R and that the energy of the free volume is equal to $E_R = 4\pi\gamma R^2$, where γ is the surface energy per unit area, almost equal to the surface energy of the liquid. According to the Boltzmann distribution, the possibility P for a macromolecule to neighbor with a hole of radius R at a certain position $\mathbf{r}$ is given by the expression:

$$P = c\exp\left[-\frac{E_R}{kT}\right] \text{ where } E_R = 4\pi\gamma R^2 \quad (4)$$

where c is a constant, k is the Boltzmann constant and T is the temperature.

The desired probability of finding a state at a position between $\mathbf{r}$ and $\mathbf{r} + \mathrm{d}\mathbf{r}$ with a hole of radius between $\mathbf{R}$ and $\mathbf{R} + \mathrm{d}\mathbf{R}$ will thus be:

$$P(\mathbf{r}, \mathbf{R})\,\mathrm{d}^3\mathbf{r}\,\mathrm{d}^3\mathbf{R} = c\exp(-E_R/kT)\mathrm{d}^3\mathbf{r}\,\mathrm{d}^3\mathbf{R} \quad (5)$$

Therefore, the mean number of states per unit volume, which have radius $\mathbf{R}$ with values between $\mathbf{R}$ and $\mathbf{R} + \mathrm{d}\mathbf{R}$ will be:

$$f(\mathbf{R})\,\mathrm{d}^3\mathbf{R} = \frac{NP(\mathbf{r},\,\mathbf{R})\mathrm{d}^3\mathbf{r}\,\mathrm{d}^3\mathbf{R}}{\mathrm{d}^3\mathbf{r}} = N\,c\exp\left(-4\pi\gamma R^2/kT\right)\,\mathrm{d}^3\mathbf{R} \quad (6)$$

where N is the number of states having positions between $\mathbf{r}$ and $\mathbf{r} + \mathrm{d}\mathbf{r}$, of which a fraction is given by the probability $P(\mathbf{r}, \mathbf{R})\,\mathrm{d}^3\mathbf{r}\,\mathrm{d}^3\mathbf{R}$.

Due to the fact that $\mathbf{R}$ does not have a preferred position in the space, function $f(\mathbf{R})$ depends only on the magnitude R of $\mathbf{R}$. Therefore, we have:

$$f(\mathbf{R}) = f(R) \quad (7)$$

Hence, the mean number of states per unit volume with radius R between R and $R + \mathrm{d}R$ is:

$$F(R)\,\mathrm{d}R = \int{}'f(R)\,\mathrm{d}^3\mathbf{R} \quad (8)$$

where the prime on the integral indicates that the integration is over all vectors $\mathbf{R}$ satisfying the condition $R < |\mathbf{R}| < R + \mathrm{d}R$, that is, over all vectors $\mathbf{R}$ that terminate in a space within a spherical cell of inner radius R and outer radius $R + \mathrm{d}R$.

Since $\mathrm{d}R$ is infinitesimal and $f(R)$ depends only on the magnitude of $\mathbf{R}$, the function $f(R)$ has essentially a constant value over the entire domain of integration, and can thus be taken outside the integral. The remaining integral represents merely the volume of a spherical cell of radius R and thickness $\mathrm{d}R$, that is, a volume equal to $4\pi R^2\,\mathrm{d}R$. Hence the previous relation becomes:

$$F(R) = N\,c\,4\pi R^2\exp\left(-\frac{4\pi\gamma R^2}{kT}\right) \quad (9)$$

The mean value of radius R can be easily extracted from Eq. 9 at the position where the first derivative of function $F(R)$ becomes zero:

$$\left.\frac{\mathrm{d}F(R)}{\mathrm{d}R}\right|_{R=\overline{R}} = 0 \Rightarrow \overline{R} = \frac{1}{2\sqrt{\pi\gamma/kT}} \quad (10)$$

Following Eq. 9, we can write in analogy, the free volume distribution function $g(V_f) = F(R)/(4\pi R^2)$:

$$g(V_f) = N\,c\,4\pi R^2\exp\left(-\frac{4\pi\gamma R^2}{kT}\right) \quad (11)$$

By setting $N = \frac{V_f}{\overline{V}_f}$, where $\overline{V}_f$ is the mean value of the total free volume V_f, and considering that constant c of Eq. 11 can be calculated taking into account that the integration of the density probability function will be equal to unity, we have:

$$\int_0^\infty g(V_f)\mathrm{d}V_f = 1 \Rightarrow c\int_0^\infty \frac{V_f}{\overline{V}_f}\exp\left(-\left[\frac{V_f}{\overline{V}_f}\right]^{2/3}\right)\mathrm{d}V_f = 1 \quad (12)$$

Equation 12 gives $c = 1/3\overline{V}_f$; therefore the probability density function is given by:

$$g(V_f) = \frac{1}{3}\frac{V_f}{(\overline{V}_f)^2}\exp\left(-\left[\frac{V_f}{\overline{V}_f}\right]^{2/3}\right) \quad (13)$$

Equation 13 is the probability density distribution function for the free volume of liquid state. Assuming further that the free volume at the equilibrium state is established into the bulk in the frozen-in process, Eq. 13 is also the probability distribution function for the free volume in the glassy state.

Let us proceed further to the state where a strain field ε has been applied to the representative volume V of the tested material subjected to plastic deformation. The regions in which this volume has been related with the largest amount of free volume will be the most probable candidate for yield transition that takes place at a critical strain $\bar{\varepsilon}$. The corresponding probability for this event to take place inside the material will be given by the following equation,

$$g(\varepsilon) = \frac{1}{3}\frac{\varepsilon}{(\bar{\varepsilon})^2}\exp\left(-\left[\frac{\varepsilon}{\bar{\varepsilon}}\right]^{2/3}\right) \tag{14}$$

where $\bar{\varepsilon}$ expresses the mean value of the distributed strain into the material. Using this equation, the number of sites that have been subjected to plastic transverse, after strain ε has been applied, is given by the following integral:

$$N(\varepsilon) = \int_0^{\varepsilon} \mathrm{d}\varepsilon\, g(\varepsilon) = \int_0^{\varepsilon} \frac{1}{3}\frac{\varepsilon}{(\bar{\varepsilon})^2}\exp\left(-\left[\frac{\varepsilon}{\bar{\varepsilon}}\right]^{2/3}\right)\mathrm{d}\varepsilon \tag{15}$$

The above-obtained integral can be used in the following for the calculation of the rate of plastic strain deformation $\dot{\varepsilon}_y$ if we assume that each site is transit at yield state by a constant rate $\dot{\kappa}$, which will be verified later in this work. The corresponding plastic strain rate equation will be given by the following equation,

$$\dot{\varepsilon}_y = \dot{\kappa}N(\varepsilon) = \dot{\kappa}\frac{1}{3}\int_0^{\varepsilon} \frac{\varepsilon}{(\bar{\varepsilon})^2}\exp\left(-\left[\frac{\varepsilon}{\bar{\varepsilon}}\right]^{2/3}\right)\mathrm{d}\varepsilon \tag{16}$$

The value of the characteristic strain $\bar{\varepsilon}$, around which the above-introduced distribution function works, is related with a specific microstructural parameter, expressing the strain above which no more elastic strain is developed.

Constitutive equations

Among the various trends, that undertake to formulate a complete set of constitutive equations for plastic behavior of materials, many different approaches have been established up to now. Some of these differences cause limited results on the related phenomena, but others are of important consequences for the whole formulation, which occasionally was attempted. One of the main differences among the various contributions concerns the multiplicative decomposition of the deformed gradient tensor $\mathbf{F}$ (Lee [26]). According to this widely accepted assumption, the tensor $\mathbf{F}$, which describes the way a material element $\mathrm{d}\mathbf{X}$ deforms in a line element $\mathrm{d}\mathbf{x}$ in the present state, is separated into the elastic and plastic parts $\mathbf{F_e}$ and $\mathbf{F_p}$ correspondingly. The two tensors lack an explicit determination in the present configuration of the material elements, because each of them is referred to different configuration states. To avoid this problem, a detailed description has been developed by Rubin [15, 16] who extended the ideas by Eckart [27] and Besseling [28]. In his work, an evolution equation has been specified including the relaxation effects of plastic deformation without introducing a plastic deformation tensor explicitly. Although Rubin's treatment has been introduced for describing a general anisotropic response of crystalline metals, his analysis can be applied as a constitutive theory for general description of the plastic behavior of materials.

According to his assumption, the elastic deformation of each material point has been formulated through a triad of vectors $\mathbf{m_i}$ $(i = 1, 2, 3)$, which are related to dilatation, distortion, and orientation of a mean atomic lattice in respect to some reference state. Since the vectors $\mathbf{m_i}$ characterize the atomic lattice in the present state, they are not directly connected to the material line elements, but they can be used explicitly as a basis for tensor referred to the present configuration as well. In the reference configuration state associated with the material, when it is stress free, this triad of vectors constitutes a set of orthonormal vectors, implying that the corresponding metric tensor m_{ij} equal to $m_{ij} = \mathbf{m_i} \cdot \mathbf{m_j}$ is given by:

$$m_{ij} = \delta_{ij} \tag{17}$$

In order to define the change of the volume element we are referred to, the dilatation J_m (which is unity in the reference lattice state) is introduced and given by:

$$j_m = \mathbf{m_1} \times (\mathbf{m_2} \cdot \mathbf{m_3}) = (\det m_{ij})^{1/2} \tag{18}$$

Moreover, to define the distortional measures of the elementary volume, Rubin has introduced another set of orthonormal vectors $\mathbf{m_i}'$ defined by the equations:

$$\mathbf{m}'_i = J_m^{-1/3}\mathbf{m_i} \text{ with } m'_{ij} = \mathbf{m_i}' \cdot \mathbf{m_j}' = J_m^{-2/3}m_{ij} \tag{19}$$

It is easily then extracted that:

$$\det m'_{ij} = 1 \tag{20}$$

The microstructural variable $\mathbf{m_i}$ is determined by an evolution equation of the form:

$$\dot{\mathbf{m}}_\mathbf{i} = \mathbf{L_m}\mathbf{m_i} \tag{21}$$

where the second order tensor $\mathbf{L_m}$ corresponds to the elastic velocity gradient and is assumed to be separated additively into the form:

$$\mathbf{L_m} = \mathbf{L} - \mathbf{L_p}, \quad \mathbf{L_p} = \mathbf{D_p} + \mathbf{W_p} \tag{22}$$

where $\mathbf{L}$ and $\mathbf{L_p}$ are the velocity gradients of total and plastic deformation, respectively, and $\mathbf{D_p}$ and $\mathbf{W_p}$ are the symmetric and antisymmetric parts of the velocity gradients that need to be specified by constitutive equations. It follows from (18), (19), (20), and (20) that

$$\frac{j_m}{J_m} = \mathbf{D}\cdot\mathbf{I}, \quad \mathbf{D}' = \mathbf{D} - \frac{\mathbf{1}}{\mathbf{3}}(\mathbf{D}\cdot\mathbf{I})\mathbf{I},$$
$$\dot{m}_{ij} = 2(\mathbf{D}' - \mathbf{D_p})\cdot(\mathbf{m_i}'\otimes\mathbf{m_i}') \tag{23}$$

where $\mathbf{D}'$ is the deviatoric part of the corresponding symmetric part $\mathbf{D}$ of the total velocity gradient tensor $\mathbf{L}$. In extracting the above relations, the plastic incompressibility

$$\mathbf{D_p}\cdot\mathbf{I} = 0 \tag{24}$$

has been used, while symbol $\otimes$ denotes the tensor product between two vectors, and $\mathbf{I}$ represents the identity tensor. The dot product $\mathbf{A}\cdot\mathbf{B}$ between two tensors denotes the usual scalar product when $\mathbf{A}$ and $\mathbf{B}$ are vectors, and it denotes the scalar $\mathrm{tr}(\mathbf{AB^T})$ when $\mathbf{A}$ and $\mathbf{B}$ are second order tensors.

Concerning uniaxial stress in the $\mathbf{e}_1$ directions in respect to a fixed rectangular Cartesian base vectors $\mathbf{e_i}$, which are parallel to $\mathbf{m_i}$, it can be shown that the velocity gradient is specified by the following form:

$$\mathbf{L} = \mathbf{D} = \frac{\dot{\alpha}}{\alpha}\mathbf{e_1}\otimes\mathbf{e_1} + \frac{\dot{b}}{b}\mathbf{e_2}\otimes\mathbf{e_2} + \frac{\dot{c}}{c}\mathbf{e_3}\otimes\mathbf{e_3} \tag{25}$$

where α, b, and c represent the stretches of the material line elements in the coordinate directions $\mathbf{e_1}$, $\mathbf{e_2}$, and $\mathbf{e_3}$, respectively, with the following initial conditions:

$$\alpha(0) = b(0) = c(0) = 1 \tag{26}$$

The antisymmetric part $\mathbf{W}$ of the velocity gradient and consequently $\mathbf{W_p}$ vanish in the case of uniaxial stress, resulting in

$$\mathbf{L_p} = \mathbf{D_p} \tag{27}$$

Then the corresponding constituents of the distortional vector $\mathbf{m_i}'$ may be represented by the following forms.

$$m'_{33} = \alpha_m^2, \quad m'_{11} = m'_{22} = \frac{1}{\alpha_m}$$
$$\mathbf{m_3}' = \alpha_m\mathbf{e_3}, \mathbf{m_1}' = \frac{1}{\sqrt{\alpha_m}}\mathbf{e_1}, \mathbf{m_2}' = \frac{1}{\sqrt{\alpha_m}}\mathbf{e_2} \tag{28}$$

where α_m is a function to be determined.

The associate flow rule, which defines the symmetric part of the plastic velocity gradient $\mathbf{D_p}$, has been written by Rubin as

$$\mathbf{D_p} = \Gamma_p\overline{\mathbf{D}}_\mathbf{p} \tag{29}$$

where Γ_p is a non-negative function expressing the rate of plastic deformation and needs to be specified, and $\overline{\mathbf{D}}_\mathbf{p}$ is the direction for plastically isotropic response, which is specified by the deviatoric portion of the driving stress tensor $\mathbf{T}'$ in the following way:

$$\overline{\mathbf{D}}_\mathbf{p} = \frac{j_m}{2\mu}[\mathbf{T}'\cdot(\mathbf{m_i}'\otimes\mathbf{m_j}')](\mathbf{m_i}'\otimes\mathbf{m_j}' - \frac{1}{3}m'_{ij}\mathbf{I}) \tag{30}$$

$$\mathbf{T}' = \mu j_m^{-1}(\mathbf{m_r}'\otimes\mathbf{m_r}' - \frac{1}{3}m'_{rr}\mathbf{I}) \tag{31}$$

with μ being the shear modulus.

For the case of uniaxial deformation, Rubin [16], solving the above equations, extracted the following expression for the time evolution of the stretch ratio α_m of the volume element, which is subjected to the imposed deformation

$$\frac{\dot{\alpha}_m}{\alpha_m} = \left[\frac{1+\frac{1-2\nu}{2(1+\nu)}\left(\frac{\alpha_m^3-1}{\alpha_m}\right)}{1+\frac{1-2\nu}{6(1+\nu)}\left(\frac{5\alpha_m^3-2}{\alpha_m}\right)}\right] \times\left[\frac{\dot{\alpha}}{\alpha} - \frac{\Gamma_p}{18}\left(\frac{\alpha_m^3-1}{\alpha_m^3}\right)(4\alpha_m^3+2)\right] \tag{32}$$

with the initial condition $\alpha_m(0) = 1$, and ν is the Poisson ratio. It must be mentioned that the stretch ratio α is equal $(1-\varepsilon)$ in compression deformation tests.

When plastic deformation is saturated, the stretch ratio $\alpha_m = \alpha_m^s$ is equal to $(1-\varepsilon_m^s)$, where ε_m^s the elastic strain at this state. The rate of elastic stretch ratio $\dot{\alpha}_m$ however at yield point is equal to zero. Assuming that the following factor at yield point is almost equal to unity,

$$\frac{18\alpha_m^3}{(\alpha_m^2+\alpha_m+1)(4\alpha_m^3+2)} \cong 1 \tag{33}$$

Then from the second part of Eq. 32, which is also equal to zero, we obtain the following equation at the saturated state,

$$\Gamma_p^s = \frac{\dot{\alpha}}{\alpha}\frac{18\alpha_m^3}{(\alpha_m^3-1)(4\alpha_m^3+2)} \cong \frac{\dot{\alpha}}{\alpha}\frac{1}{\alpha_m^s-1} \tag{34}$$

In the previous section of the presented model, however, we obtained the integral Eq. 16 for the rate of plastic deformation emerged into the deformed material; this fact leads to the following expression for Γ_p:

$$\Gamma_p = \dot{\varepsilon}_y = \dot{\kappa}N(\varepsilon) = \dot{\kappa}\int_0^\varepsilon \frac{1}{3}\frac{\varepsilon}{(\overline{\varepsilon})^2}\exp\left(-\left[\frac{\varepsilon}{\overline{\varepsilon}}\right]^{2/3}\right)\mathrm{d}\varepsilon \tag{35}$$

The unknown factor $\dot{\kappa}$ of the above equation can be now calculated from the limited case of plastic saturation, given that at this state the integral of Eq. 35 is equal to unity,

$$\Gamma_p^s = \frac{\dot{\alpha}}{\alpha}\frac{1}{\alpha_m^s-1} = \dot{\kappa}\cdot 1 \tag{36}$$

Combining Eqs. 35 and 36, we obtain the following expression for the rate of plastic deformation:

$$\Gamma_p = \frac{\dot{\alpha}}{\alpha}\frac{1}{\alpha_m^s-1}\int_0^\varepsilon \frac{1}{3}\frac{\varepsilon}{(\overline{\varepsilon})^2}\exp\left(-\left[\frac{\varepsilon}{\overline{\varepsilon}}\right]^{2/3}\right)\mathrm{d}\varepsilon \tag{37}$$

As it is clear from the above equation, there in no strain rate and temperature dependence of plastic deformation,

given that we avoid the concept of thermal activated process in our analysis. To overcome this shortcoming, we proceed to the next section introducing the viscoelastic behavior as a main part of the constitutive description.

Strain rate and temperature dependence of yield stress in polymers

The experimental yield stress in polymer solids depends strongly on the strain rate deformation. It increases also as the temperature is lowered or the hydrostatic pressure is raised. On the other hand, when a constant strain below yield point is applied on amorphous polymers, the material undergoes a non-linear viscoelastic behavior with a terminal stress for $t \to \infty$ below yield stress as well. These observations can give the impression that yield phenomenon in polymers is fundamentally different from that in metals that follow the yield criteria, and that it might be a special and unique non-linear viscoelastic effect. Regarding the length scale of these viscoelastic and viscoplastic phenomena, some differences also are recorded, given that the characteristic size of shear bands associated with plastic phenomena is of the order of some micrometers [29, 30] that exceeds three orders of magnitude the characteristic length of pure viscoelastic effect. What is true however is that these two phenomena coexist in the mechanical behavior of polymers [5], and it is a matter of total strain and strain rate applied on the material that decides which of these two effects will prevail in respect to the other one. Matsuoka [31], who describes this behavior systematically in a relevant book "Relaxation Phenomena in Polymers," comes to the result that there is a critical strain ε^* which controls the viscoplastic response of glassy polymers. When the strain rate $\dot{\varepsilon}$ is slow ($\dot{\varepsilon}\lambda_i < \varepsilon^*$ where λ_i is a set of relaxation modes describing the viscoelastic behavior of polymers), the yield stress σ_y is never reached, and the final steady state stress is that of linear viscoelasticity $E_i\lambda_i\dot{\varepsilon}$, with E_i being the moduli of the corresponding modes. If the material exhibits no stress overshoot in the yield stress, then $\varepsilon^* = \dot{\varepsilon}\lambda_i$, and the steady state stress is equal to the yield stress σ_y. When stress overshoot is observed, which is common in most glassy polymers, $\varepsilon^* < \dot{\varepsilon}\lambda_i$, and beyond yielding, a transition takes place with a new structure in the material state, resulting in a new smaller value of λ_i, which is equal to $\varepsilon^*/\dot{\varepsilon}$.

After a more detailed analysis, Matsuoka concluded that strain magnitude is a crucial factor in determining whether the viscoelastic or plastic path is followed. Regardless of transient or steady state conditions, it depends on whether $\varepsilon < \varepsilon^*$ or $\varepsilon > \varepsilon^*$.

This behavior according to Matsuoka can be approximated by a single equation:

$$\sigma = E\varepsilon^*\left[1 - \exp\left(-\frac{\varepsilon}{\varepsilon^*}\right)\right] \tag{38}$$

Moreover, describing in detail the strain rate and temperature dependence of this viscoplastic stress, Matsuoka extracted some scaling rules working very accurately in each corresponding case. According to the first rule, a stress–strain curve at $\dot{\varepsilon}_2$ can be predicted from an experimental stress–strain curve at strain rate $\dot{\varepsilon}_1$ by multiplying the stress and strain, in the experimental curve by the scaling factor $(\dot{\varepsilon}_2/\dot{\varepsilon}_1)^n$ and $(\dot{\varepsilon}_2/\dot{\varepsilon}_1)^m$ for the stress and strain, respectively, where n and m are the corresponding exponents of the power law describing the non-linear viscoelastic effects. In the case of polycarbonate, Matsuoka used the values $n = 0.035$ and $m = 0.023$ to fit the experimental data, but their exact values for various polymers is always possible from the rate dependence of yield stress.

The temperature dependence of yield stress in Matsuoka's analysis has been given by a second scaling rule resulting in a simple equation relating the temperature with the shear modulus of most polymers as follows:

$$G_2/G_1 = \left(1 - \frac{T_2}{T_c}\right)/\left(1 - \frac{T_1}{T_c}\right) \tag{39}$$

where T_c is a critical high temperature up to 50 °C larger than glass transition temperature ($T_c \geq T_g$) at which the yield stress vanishes ($\sigma_y = 0$).

G_2 and G_1 are the unrelaxed shear modulus of the polymer at the corresponding temperatures T_2 and T_1, respectively. This relation has been extracted by Matsuoka [31] using the energy balanced equation at yield point for the strain free energy under uniaxial extension, and the measurements of enthalpy increased (ΔH) at the same point. The corresponding entropy increase (ΔS) is obtained by the fact that strain free energy ($\Delta H - T\Delta S$) is zero at temperature T_c, which extrapolates to $\sigma_y = 0$.

By using these two scaling rules for the strain rate and temperature dependence of yield effect, and the subsequent constitutive analysis presented above, we can describe in detail the yield and post-yield phenomena of polymers. In the following section, we will use typical experimental results for various polymers existing in bibliography, and the solution of related equations to compare our theory with previous works.

Experimental verification

The theoretical model developed in this work leads to the prediction of the entire yield behavior of amorphous polymers, including yield stress, strain softening, strain rate effect and temperature dependence exhibited by the materials.

For the prediction of the yield stress, the only parameters that are necessary in solving the subsequent equations are the Young modulus and the three parameters $(\bar{\varepsilon}, \varepsilon^*, \alpha_m^s)$, which appeared in Eq. 37 of the plastic rate deformation Γ_p. The estimation of the critical strain magnitude ε^* can be made through the free volume amount of the tested material.

Following a plausible assumption that when yield transition is generated inside a box of un-deformed volume V_0 containing the fraction free volume v_f, the total change of its volume ΔV will be given by the simple equation:

$$v_f = \Delta V/V_0 = \varepsilon^* 3\mathrm{K}/E \tag{40}$$

where K and E are the bulk and elasticity modulus of the material, the corresponding strain yield ε^* where maximum stress is appeared can be easily estimated as follows:

$$\varepsilon^* = \hat{v}_f\, E/3\mathrm{K} = \hat{v}_f/(1-2v) \tag{41}$$

To obtain the above estimation, we have assumed that during plastic deformation a part of the matter around free volume is moved in a suitable way into these cavities. Small amount of the total volume should then be detected, as has been verified in many experiments, Spitzing and Richmond [32].

The elastic stretch ratio α_m^s at saturated state can be simply determined by the value of stress σ^sat the same state,

$$\alpha_m^s - 1 = \frac{\sigma^s}{E} \tag{42}$$

The strain softening effect does not need any more assumption, and it is revealed simply from the solution of constitutive equations. The strain rate and temperature dependence effect could be described easily by using the two scaling rules presented in the previous context, and the fitting of the two parameters n and T_2 from the experimental data in each special material separately.

As tested materials we will take into account three of the most common amorphous polymers, (PMMA, PC, and PS), which have been widely studied in recent years by many authors for checking relevant theories for plastic behavior in polymers. Among the works existing in bibliography, there are many data for such materials, for a lot of experiments under various modes of deformation, thermal treatment, and loading rates were published by Hasan and Boyce [6–8]. Among these tests, we will use compression loading experiments in avoiding geometrical instabilities obscuring the strain softening effect.

Starting with PMMA, we reproduce from the relevant work by Hasan and Boyce [7] in Figs. 1a and 2a the results of isothermal constant strain rate, for uniaxial compression tests on annealed and quenched PMMA at two different temperatures. The essential features of the typical yield and post-yield effect are observed in these experiments. The initial elastic behavior followed by a non-linear viscoelastic response reaches a maximum stress and an isothermal material softening after that resulting in a steady flow stress. The dependence of yield stress on strain rate and temperature is obvious from these plots, while the reduction of stress values for the quenched materials in respect to the annealed ones is also revealed from the comparison of the corresponding curves between the two figures.

Figures 1 and 2 show the corresponding plots as they have been calculated from the present theory. More specifically, the integration of Eq. 32 determines the value of stretch ratio α_m at every state of deformation, by incorporating the corresponding magnitude of strain into the viscoelastic constitutive Eq. 38, and the calculation of stress can be made. The integration has been made numerically, using small time steps, with the software *Mathematica* 4, developed by Wolfram [33], and a personal computer. Gradually decreasing the original time step up to one tenth, a high convergence has been obtained. In each step of integration, the calculation of plastic strain rate is obtained by Eq. 37. Summarizing, the parameters that are necessary to model the experimental data are as follows: Parameter ε^* is directly related with the mean size of

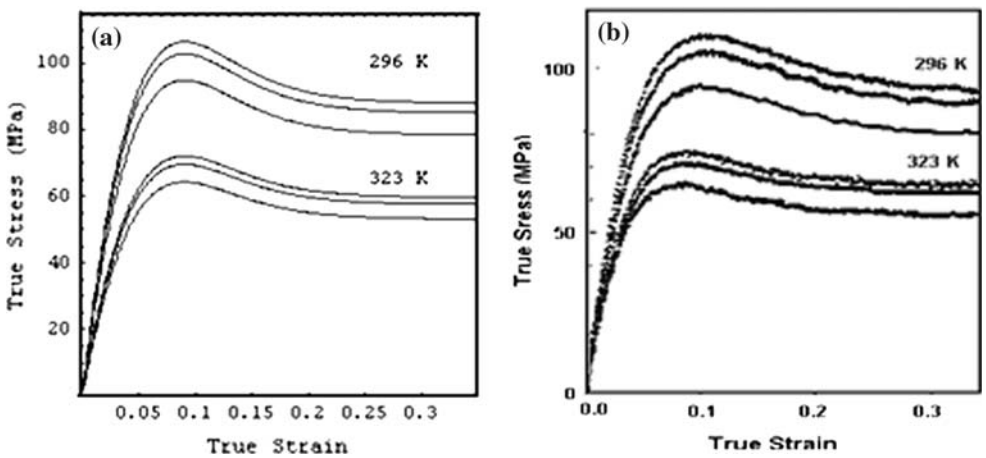

Fig. 1 (**a**) Calculated plots for annealed PMMA specimens deformed to different (%) applied strains (scan rates, −0.001, −0.0005, −.0001 s^{-1}) at temperatures 296 K and 323 K. (**b**) Experimental plots for annealed PMMA specimens deformed to different (%) applied strains (scan rates, −0.001, −0.0005, −.0001 s^{-1}) at temperatures 296 K and 323 K (Reproduced from Hasan and Boyce, Ref. [7])

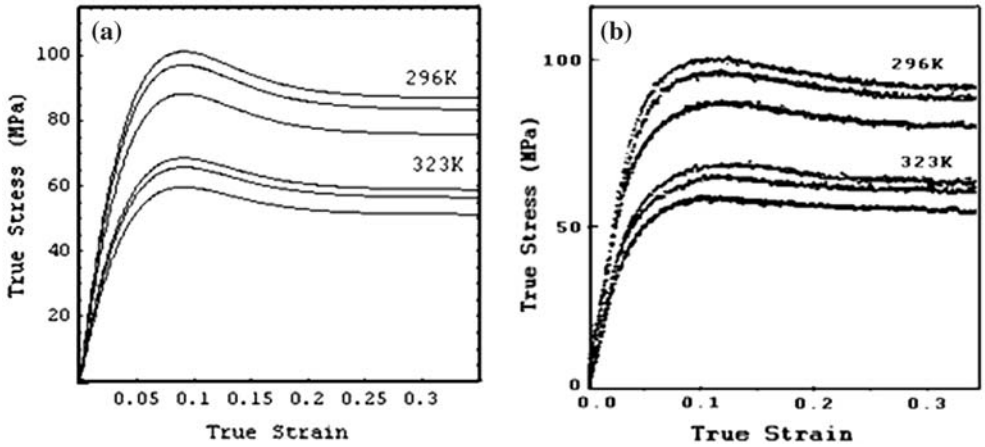

Fig. 2 (**a**) Calculated plots for quenched PMMA specimens deformed to different (%) applied strains (scan rates, −0.001, −0.0005, −.0001 s^{-1}) at temperatures 296 K and 323 K (**b**) Experimental plots for quenched PMMA specimens deformed to different (%) applied strains (scan rates, −0.001, −0.0005, −.0001 s^{-1}) at temperatures 296 K and 323 K (Reproduced from Hasan and Boyce, Ref. [7])

various types of defects. It can be estimated independently from free volume measurements with various techniques. In our case it was fitted for the better description of experimental curves. Parameter $\bar{\varepsilon}$ expresses the mean value of the distributed strain into the material. As discussed earlier, this parameter value is similar to the saturated elastic strain $1 - \alpha_s^m$. The quantity α_s^m is the saturated stretch ratio and the corresponding saturated strain is obtained by dividing the almost stable value of stress, establishing after strain softening, by the apparent modulus in the post-yield region, before strain hardening occurs. Parameter n is a fitting constant, to capture the strain rate effect. So, the basic constants for the modeling of yield response are the quantities $\bar{\varepsilon}$ and ε^*.

Table 1 contains the values of parameters used in the corresponding calculations where the magnitude of the elastic constants (E, v) has been taken from the corresponding work by Hasan and Boyce [6–8]. In order to obtain the reduced stress values of the quenched materials of Fig. 2, we assumed that the corresponding reduction of the controlling parameter ε^* is due to the reduction of bulk modulus for such specimens given that larger amounts of free volume will be frozen inside quenched materials when the temperature is suddenly changed, Hasan et al. [7]. By comparing the experimental and calculated plots shown in Figs. 1a, b and 2a, b for the case of annealed and quenched PMMA specimens, we conclude that a strong evidence is raised for the plausible assumptions of this work in describing the yield phenomenon of amorphous polymers.

We proceed now to examine how this model works on similar data for another amorphous polymer like PS. Experimental results under compression loading for this glassy polymer are also published by Hasan and Boyce [8] together with similar tests for PMMA and PC. In this work, systematic measurements have been executed on annealed and quenched materials deformed in compression to various levels accompanied by differential scanning calorimetric (DSC) tests on the unloading specimens. The DSC scans release the change of specimen enthalpy when heating at constant rate and lead to a very good insight into the evolution of material state with inelastic straining.

In Fig. 3a, we reproduce the stress–strain plots for the annealed and quenched PS at the temperature 296 K and compression loading at strain rate −0.001 s^{-1}. Comparing these plots with the corresponding curves of Figs. 1a and 2a for PMMA at the same temperature and strain rate, we notice the differences in the maximum yield stresses (110 MPa for PMMA and 92 MPa for PS). By plotting in Fig. 3 the corresponding stress–strain curves as have been calculated using the presented model, this difference can be analyzed by comparing the parameters used in integrating the constitutive equations. Table 2 presents the elastic constants and the subsequent parameters used in the relevant calculations for the case of PS. In Fig. 3a and b, the experimental and theoretical results for the case of PS are also presented, exhibiting again the appropriateness of the presented model for yield phenomenon in polymers.

If we proceed now to the case of PC as another example for the validity of the presented theory, we will use the experimental data from a relative work by Boyce and Arruda [34], concerning cylindrical compression specimens

Table 1 Model parameter values for annealed and quenched PMMA

Sample	E (MPa)	v	ε^*	$\bar{\varepsilon}$	a_m^s	n	T_c (K)
Annealed	2,300	0.3	0.10	0.03	1.03	0.05	379
Quenched	2,300	0.3	0.08	0.03	1.03	0.05	379

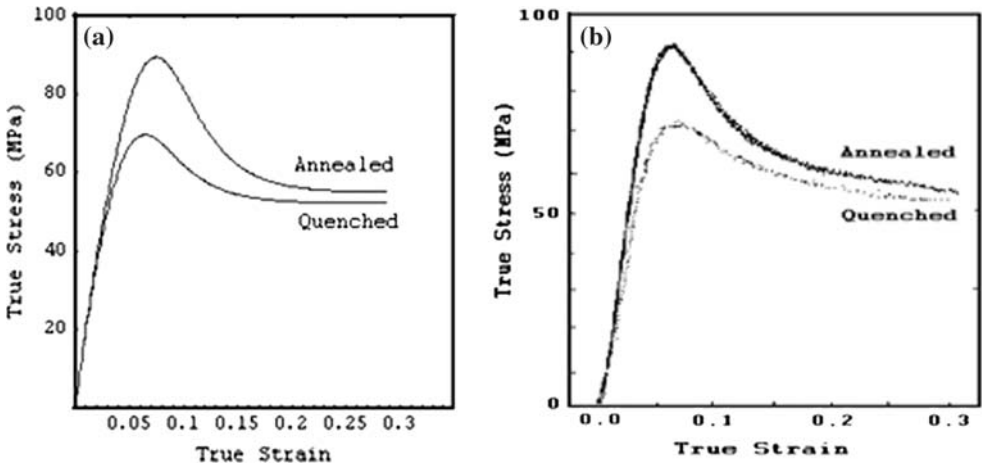

Fig. 3 (**a**) Calculated plots for annealed and quenched PS specimens deformed to different (%) applied strains (scan rate, $-0.001\ s^{-1}$) at temperature 296 K. (**b**) Experimental plots for annealed and quenched PS specimens deformed to different (%) applied strains (scan rate, $-0.001\ s^{-1}$) at temperature 296 K (Reproduced from Hasan and Boyce, Ref. [6])

Table 2 Model parameter values for annealed and quenched PS

Sample	E (MPa)	v	ε^*	$\bar{\varepsilon}$	a_m^s	n
Annealed	3,000	0.3	0.070	0.02	1.02	0.05
Quenched	3,000	0.3	0.060	0.02	1.02	0.05

subjected to five different strain rates ranging from 1.0 s^{-1} to 0.0001 s^{-1}. The constant strain rates, and the large compression strains up to 125% obtained at room temperature for the examined PC, reveal very clearly a planar molecular orientation process, which results in the strain hardening effect under the loading conditions. To obtain the complete calculation of the stress under these conditions, including this stage of deformation, a supplementary term for stress should be taken into account due to the entropic hardening. Modeling of strain hardening has been an interesting issue. A lot of approaches have been introduced, and it is worth mentioning some interesting works introduced by Hoy and Robbins [35–37], which offer a deep understanding of this effect. In our case, the three-chain model of James and Guth [38] has been used. In this way, the total stress may be expressed as

$$\sigma_{\text{total}} = \sigma + \sigma_h \tag{43}$$

where σ is obtained by solving the system of constitutive equations as in the previous cases, and σ_h is a stress attributed to the strain hardening and is given by

$$\sigma_h = G_r \frac{\sqrt{N}}{3}\left[\lambda_i L^{-1}\left(\frac{\lambda_i}{\sqrt{N}}\right) - \frac{1}{3}\sum_{j=1}^{3}\lambda_j L^{-1}\left(\frac{\lambda_j}{\sqrt{N}}\right)\right] \tag{44}$$

where L^{-1} is the inverse Langevin function, λ_i are the stretch ratios in the three principal directions, with $\lambda_1 = \alpha - \alpha_m$ and $\lambda_2 = \lambda_3 = 1/(\alpha - \alpha_m)^{0.5}$ and N is the equivalent number of rigid links between entanglements. As is mentioned by Boyce et al. [34], $\sqrt{N}$ is equal to the terminal or locking stretch. From the true stress–strain curves of Fig. 4a, locking occurs at a strain almost equal to 1.25, resulting in a value for N approximately equal to 1.8. G_r is the strain hardening modulus, taken to be equal to 5 MPa.

The theoretical results of stress versus strain, for the five strain rates at compression loading, are plotted in Fig. 4, and the corresponding used parameters are listed in Table 3.

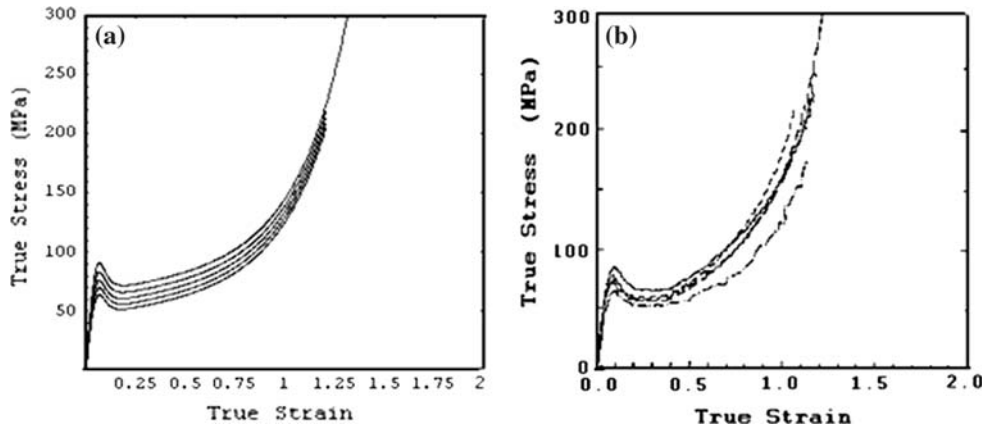

Fig. 4 (**a**) Calculated plots for PC specimens deformed to different (%) applied strains (scan rates, -1, -0.1, -0.01, -0.001, $-0.0001\ s^{-1}$) at temperature 296 K. (**b**) Experimental plots for PC specimens deformed to different (%) applied strains (scan rates, -1, -0.1, -0.01, -0.001, $-0.0001\ s^{-1}$) at temperature 296 K (Reproduced from Boyce and Arruda, Ref. [34])

Table 3 Model parameter values for PC

E (MPa)	v	ε^*	$\bar{\varepsilon}$	a_m^s	n
2,300	0.3	0.10	0.02	1.02	0.04

Conclusions

In this work, an attempt has been made to understanding the fundamental manner by which glassy polymers yield, under mechanical deformation process. The concept of free volume, which has been used many times in the past, enlightening this phenomenon, has been reconsidered in the presented model but in a different way. The change of both free volume mean value and the free volume distribution, in respect to deformation, has been experimentally verified [25] for glassy polymers. In the present work, as a first approximation, this fact is not taken into account. This fact will be analyzed in a future work. Here, we do not emphasize on free volume changes during deformation process as a possible mechanism for explaining the reduction of the material resistance under loading conditions, but we use the free volume distribution as the origin for strain localization and strain non-uniformity under loading state. The formulation of this inhomogeneity by a distribution density function results in a plausible explanation of the plastic behavior in polymers. The fact that the yield process does not appear suddenly on the loading material, but it takes part progressively coexisting with viscoelastic deformation, is a serious evidence that it is generated in various positions spread inside the matter around localized states, Olenik [39]. The manner by which the plastic deformation proceeds is a matter of the amount of these sites, that take part during the evolution of the yield effect. Consequently, the necessity of a distribution function for these sites is then plausible for describing the rate by which the plastic deformation proceeds. On the other hand, the existence and the degree of strain non-uniformity vary from polymer to polymer, and further can be modified by temperature, strain rate, and history. These events, which have been experimentally verified for the materials considered in this work (PMMA, PS, and PC), are taken into account for the quantitative description of yield stress and strain softening, exhibited under most conditions in polymer glasses.

What is worth emphasizing in this analysis is the fact that strain softening effect, which is a direct result of strain non-uniformity, is captured because we avoid the calculation of the plastic deformation gradient tensor as usually done in the context of plasticity theories of polar decomposition for the total deformation gradient. This determination would oblige us to integrate the associated flow rule equation across all reference gauge length assuming a uniform distribution of plastic events into the material, and consequently obscuring the main assumption of strain non-uniformity. In contrast to this approach, the kinematic formulation introduced by Rubin avoids this determination by concentrating on rate evolution equations for variables established on a micromechanical base. Under such a description, the yield phenomenon takes part when the rate deformation per unit strain becomes equal to plastic deformations emerged into the loaded material.

References

1. Bowden PB, Raha S (1974) Philos Mag 29:146. doi:10.1080/14786437408213560
2. Robertson RE (1966) J Chem Phys 44:3950. doi:10.1063/1.1726558
3. Argon AS (1973) Philos Mag 28:839. doi:10.1080/14786437308220987
4. G'Sell C, Jonas JJ (1981) J Mater Sci 14:583
5. Boyce MC, Parks DM, Argon AS (1988) Mech Mater 7:15. doi:10.1016/0167-6636(88)90003-8
6. Hasan OA, Boyce MC (1993) Polymer (Guildf) 34:5085. doi:10.1016/0032-3861(93)90252-6
7. Hasan OA, Boyce MC (1995) Polym Eng Sci 35:331. doi:10.1002/pen.760350407
8. Hasan OA, Boyce MC, Li XS, Berko S (1993) J Polym Sci Phys 31:185. doi:10.1002/polb.1993.090310207
9. Eyring HJ (1936) J Chem Phys 4:283. doi:10.1063/1.1749836
10. Dlubek G, Bondarenko V, Pionteck J, Supej M, Wutzler A, Krause-Rehberg R (2003) Polymer (Guildf) 44:1921. doi:10.1016/S0032-3861(03)00056-9
11. Schmidt M, Maurer FHJ (2000) Polymer (Guildf) 41:8419. doi:10.1016/S0032-3861(00)00181-6
12. Kanaya T, Tsukushi T, Kaji K, Bartos J, Kristiak J (1999) Phys Rev E Stat Phys Plasmas Fluids Relat Interdiscip Topics 60(2):1906. doi:10.1103/PhysRevE.60.1906
13. Higuchi H, Yu Z, Jamieson AM, Simha R, McGervey JD (1995) J Pol Sci B: Polym Phys 33:2295. doi:10.1002/polb.1995.090331701
14. Xiao-Yan Wang KM, Lee Y, Stone MT, Sanchez IC, Freeman BD (2004) Polymer (Guildf) 45:3907. doi:10.1016/j.polymer.2004.01.080
15. Rubin MB (1994) Int J Solids Struct 31(19):2615. doi:10.1016/0020-7683(94)90222-4
16. Rubin MB (1994) Int J Solids Struct 31(19):2635. doi:10.1016/0020-7683(94)90223-2
17. Spathis G, Kontou E (1998) Polymer (Guildf) 24:189
18. Spathis G, Kontou E (1999) J Appl Polym Sci 71:2007. doi:10.1002/(SICI)1097-4628(19990321)71:12<2007::AID-APP10>3.0.CO;2-W
19. Wendorff JH, Fisher EW (1973) Kolloid Z Z Polym 251:876. doi:10.1007/BF01498914
20. Curro JJ, Roe RJ (1984) Polymer (Guildf) 25:1424. doi:10.1016/0032-3861(84)90104-6
21. Roe RJ, Curro JJ (1983) Macromolecules 16:428. doi:10.1021/ma00237a018
22. Williams ML, Landel RF, Ferry JD (1955) J Am Chem Soc 77:3701. doi:10.1021/ja01619a008
23. Malhotra BD, Pethrick RA (1983) Eur Polym J 19:45. doi:10.1016/0014-3057(83)90193-3
24. Malhotra BD, Pethrick RA (1983) Polymer (Guildf) 24:165

25. Goyanes S, Rubiolo G, Salgueiro W, Somoza A (2005) Polymer (Guildf) 46:9081. doi:10.1016/j.polymer.2005.07.020
26. Lee EH (1966) Elastic–plastic deformation at finite strain. J Appl Mech 36:1
27. Eckard C (1984) Phys Rev 73:373. doi:10.1103/PhysRev.73.373
28. Besseling JF (1968) In: Proceedings of IUTAM symposium on irreversible aspects of continuum mechanics, Vienna, Springer, pp 16–53
29. Chau CC, Blackson J (1995) Polymer (Guildf) 36:2511. doi:10.1016/0032-3861(95)91195-D
30. Anglan H, El-Hadik GY, Faughnan P, Bryan C (1999) J Mater Sci 34:83. doi:10.1023/A:1004465507788
31. Matsuoka S (1992) Relaxation phenomena in polymers, 2nd edn. Hanser, Ch. 3
32. Spitzing WA, Richmon O (1979) Polym Eng Sci 19:1129. doi:10.1002/pen.760191602
33. Wolfram SS (1993) Mathematica, a system for doing mathematics by computer, 2nd edn. Wolfram Research, New York
34. Boyce MC, Arruda EM (1990) Polym Eng Sci 30(20):1288. doi:10.1002/pen.760302005
35. Hoy RS, Robbins MO (2008) Phys Rev E Stat Nonlin Soft Matter Phys 77:031801. doi:10.1103/PhysRevE.77.031801
36. Hoy RS, Robbins MO (2007) Phys Rev Lett 99:117801. doi:10.1103/PhysRevLett.99.117801
37. Hoy RS, Robbins MO (2006) J Pol Sci B: Polym Phys 44:3487. doi:10.1002/polb.21012
38. James HM, Guth E (1943) J Chem Phys 11:455. doi:10.1063/1.1723785
39. Oleynik EF (1990) In: Baer E, Moet S (eds) High performance polymer. Munchen, Ch., 4, p 80